Potentially Automated Mechanical Characterization of Metal Components by Means of Hardness Test Complemented by Non-Contact 3D Measurement

To cite this article: Gabriella Bolzon 2022 *J. Phys.: Conf. Ser.* **2293** 012010

Journal of Physics: Conference Series **2293** (2022) 012010 doi:10.1088/1742-6596/2293/1/012010

Potentially Automated Mechanical Characterization of Metal Components by Means of Hardness Test Complemented by Non-Contact 3D Measurement

Gabriella Bolzon

Department of Civil and Environmental Engineering, Politecnico di Milano, 20133 Milano, Italy

gabriella.bolzon@polimi.it

Abstract. Metal structures and infrastructures subjected to demanding working conditions must be carefully monitored throughout their entire life cycle. In fact, high operating temperatures and interaction with aggressive environments produce significant variation of the mechanical characteristics of the materials, and eventually compromise the overall structural integrity. The evolution over time of metal properties can be determined in fast, cheap and non-destructive manner by hardness tests, processing the data that describe the geometry of the residual deformation left on the indented surface. The required equipment can be mounted on the arms of collaborative robots, and/or on frames that move on wheels or rails, to detect the material characteristics automatically, over large distances and with high spatial resolution. The reliability of such a diagnostic approach depends on the accuracy of the information that can be collected, in situ, by portable devices that perform 3D contactless measurement, and on the robustness of the data filtering and interpretation procedures. These issues are illustrated in this contribution.

1. Introduction

Important structures and infrastructures for energy production and transportation are made by the assembly of simple metal components. This is for instance the case of pipeline networks, windmill farms and offshore platforms, which represent large mechanical systems subjected to demanding working conditions [1]-[4].

High operating temperatures and interaction with aggressive environments produce significant variation of the mechanical characteristics of the materials, and eventually compromise the overall structural integrity. Partial replacement of elements due to local failures, e.g. induced by accidents and fires, modifies the safety factors foreseen in the design phase, and their spatial distribution.

The evolution over time of the local metal properties can be determined in fast, cheap, and non-destructive manner by hardness tests [5], processing the data that describe the geometry of the residual deformation left on the indented surface [6]. The experimental work can be performed on site, on the exercised components, with no need to extract and to machine specimens, by the use of portable durometers and mapping tools [7]. The equipment can be mounted on the arms of collaborative robots, and/or on frames that move on wheels or rails to detect the material characteristics automatically, over large distances and with high spatial resolution. The collected data can be transferred through virtual network to facilitate the structural integrity control over the entire lifetime of components even difficult to access.

The reliability of this diagnostic approach depends on the accuracy of the information that can be collected in situ, and on the robustness of the data filtering and interpretation procedures. These issues are illustrated in this contribution.

2. Diagnostic analysis

Hardness tests simply consist of pressing a tip made of hard steel or diamond against the surface of the investigated material sample. In metals, this action produces a permanent deformation, for instance shown in figure 1. The geometry of this residual imprint can be acquired by various portable devices. One option is provided by optical microscopes with variable focal length that perform non-contact 3D measurements.

The output of this kind of instruments, already available on the market, is shown in figure 2. The graph visualizes the imprint produced by the axisymmetric sphero-conical Rockwell tip pressed against the surface of pipeline steel at 2 kN maximum load [8].

The 3D map in figure 2 represent the performed measurements in the local reference system, defined by the indented plane and by the symmetry axis of the residual imprint. The picture displays the axisymmetric deformation produced by an axisymmetric indenter in isotropic metals. The graph also evidences that the imprint portion below the reference plane reproduces the geometry of the penetrating tip.

Figure 1. Residual deformation produced by indentation tests on pipeline steel.

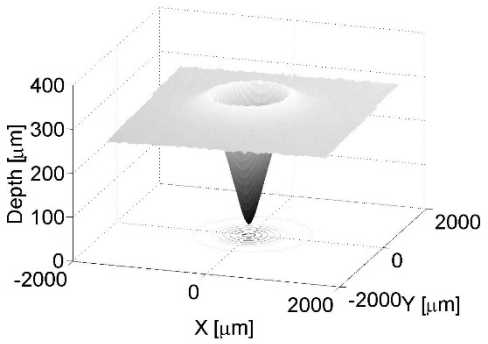

Figure 2. Map of the residual imprint left by Rockwell indentation on pipeline steel at 2kN force [7].

The geometry of the residual deformation is rich in information on the constitutive properties that govern the plastic flow in the considered material. The corresponding parameter values can be recovered through inverse analysis procedures based on the numerical simulation of the test, usually performed by finite element (FE) analysis.

Figure 3 shows the FE model of the Rockwell test, while a typical simulation output is represented in figure 4. The geometry of the computed profile depends on the material parameters provided as input in the FE analysis, in particular on the values of the elastic limit and of the material strength. The actual values of these properties are then determined by the minimization of the discrepancy between the experimental measurements and the corresponding computed quantities. The details of the parameter calibration procedure are illustrated in [7].

3. Imprint mapping

The imprint mapping represents an essential ingredient of the material calibration methodology considered here. The effectiveness of this information source has been verified in previous work, concerning different metals tested at a few kN load.

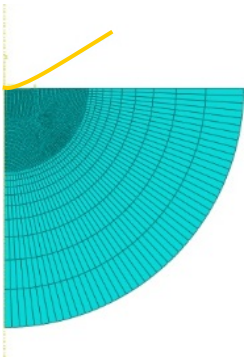

Figure 3. Finite element (FE) model of the axis-symmetric Rockwell indentation test.

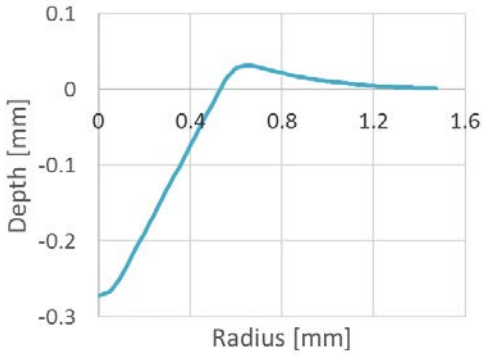

Figure 4. The profile of the residual imprint produced by Rockwell indentation on pipeline steel, obtained by FE simulation.

Automation can be facilitated by the consideration of smaller applied forces, which implies a substantial reduction of the overall dimensions and weight of the equipment to be used on site. Thus, the size of the residual imprint is also reduced, and so are the image acquisition times. However, the smaller dimensions of the mapped region emphasize the roughness of the indented surface and the presence of local defects. Also, the automatic setup of the measurement system may not be optimized for all ambient conditions in investigations performed in situ.

Some experimental disturbances are for instance evidenced in figures 5 and 6. The pictures (top views) and the 3D graphs visualize the consequences of the Rockwell tests performed on pipeline steel for 150-200 N applied force, consistent with superficial hardness tests according to ASTM E18–20 Standard classification [9]. The data were acquired with the same instrumentation (Alicona IF) used to reproduce the deformation represented in figure 2.

The 3D maps show common noises associated with the considered optical imaging device. In particular, figure 5 shows the reflection peaks produced by the pressed bottom of the imprint, which acquires the characteristics of a mirror. On the other side, figure 6 shows that some information may be lost when the light intensity is reduced. These inconveniences cannot be fully ruled out when relying on automatic measurement systems, but most disturbances can be controlled by processing the raw collected data as described here below.

The geometry of the deformation produced by Rockwell indentation in the isotropic metals is expected to be axis-symmetric. Therefore, attention can be focused on a pre-selected number of the cross sections of the entire imprint. Those selected in the present work are placed in correspondence of eight radial directions equally rotated (by 45 degrees) with respect to each other.

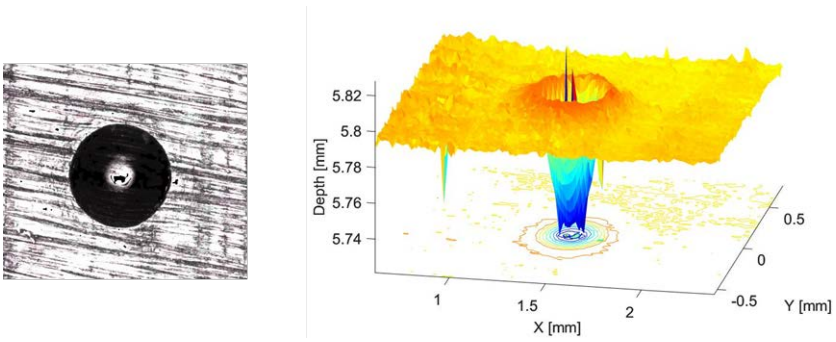

Figure 5. Top view and reconstructed geometry of imprint A, 200N applied force.

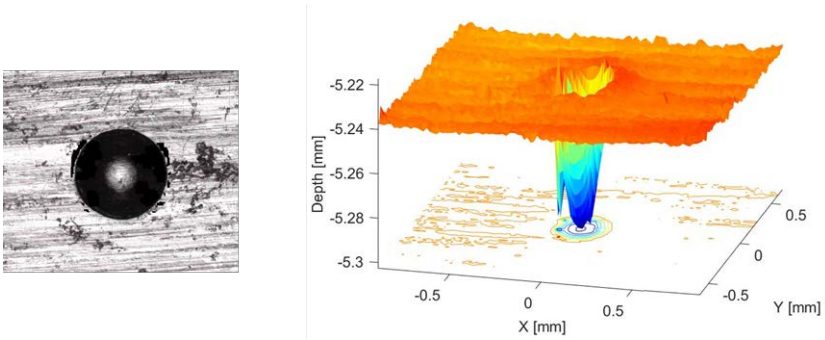

Figure 6. Top view and reconstructed geometry of imprint B, 150 N applied force.

Figure 7 and figure 8 visualize the radial cross section extracted from the maps of figure 5 (imprint named A) and figure 8 (imprint B).

The information content of the retained measurements can be evaluated by proper orthogonal decomposition (POD) [10]. Figure 9 shows the first bases of the POD representation of imprint A. The first mode (red curve) consists of the (scaled) mean permanent deformation, in this case affected by the systematic presence of light peaks reflected from the bottom of the imprint, see figure 7. The other bases mainly contain white noise.

In all cases, the main disturbances affect the region situated below the original level of the indented plane. On the other hand, this noisy portion of the deformed surface is expected to reproduce the shape of the sphero-conical Rockwell tip, with 120° opening angle and rounded end with 200 μm radius. This characteristic feature can be used to reduce the experimental disturbances. One possible filtering procedure consists in neglecting all the image points, which are located outside a band of pre-defined width (say, δ) over and below the ideal Rockwell profile.

Figure 10 displays the mean profile and the confidence limits of imprint A recovered by filtered data, assuming 5μm tolerance δ. The graphs highlight the roughness of the metal surface, but the average curve is well defined. This result is particularly meaningful since the piling up portion of the residual deformation is known to reflect with the highest sensitivity the material characteristics that govern the plastic flow [11].

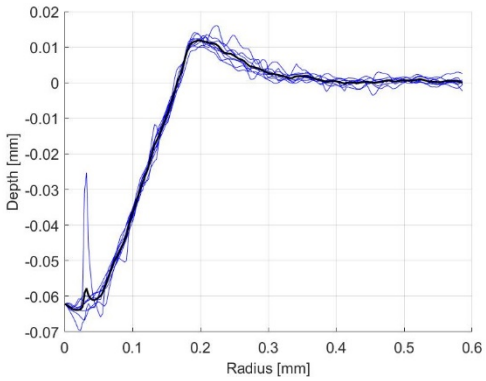

Figure 7. Radial cross section extracted from the 3D map of imprint A (blue thin lines), and the corresponding mean profile (black).

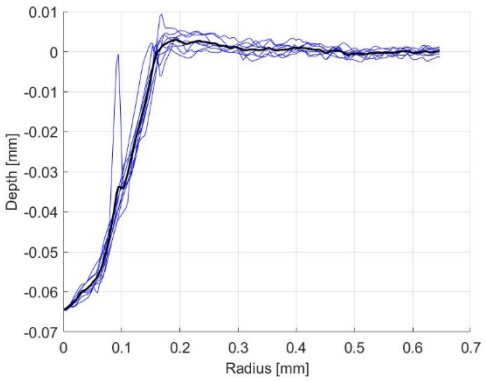

Figure 8. Radial cross section from the 3D map of imprint B (blue thin lines), and the corresponding mean profiles (black).

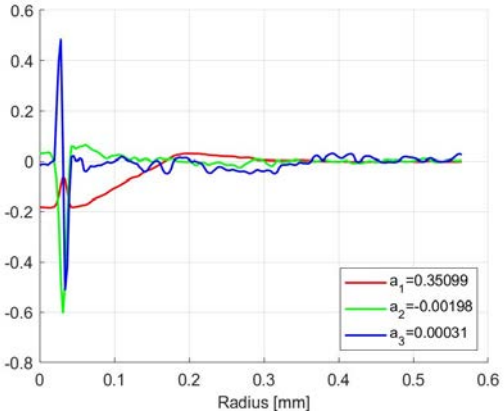

Figure 9. The first three POD bases associated to imprint A.

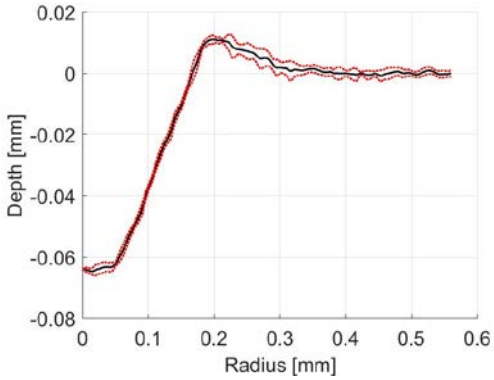

Figure 10. Mean profile and confidence limits of imprint A, filtered data.

4. Closing remarks

This contribution focuses on the non-contact measurement of the permanent deformation left on metals by hardness tests. This geometrical information can be exploited for diagnostic purposes, to identify the current mechanical properties of exercised components difficult to access and subjected to demanding working conditions.

The accuracy and reliability of data collected by portable equipment has been verified for load levels consistent with superficial hardness tests according to ASTM E18–20 Standard classification. This choice improves the portability of equipment to be used on site and reduces the mapping times, making it feasible to investigate large structural systems such as pipeline networks, windmill farms and offshore platforms, potentially in a fully automated way.

References

[1] Bolzon G, Gabetta G and Nykyforchyn H (eds.) 2020 *Degradation Assessment and Failure Prevention of Pipeline Systems*, Lecture Notes in Civil Engineering, vol. 102, Springer.
[2] Sherif SA, Barbir F and Veziroglu TN 2005 *Solar Energy* **78** 647–60
[3] https://www.eastcountymagazine.org/dark-side-%E2%80%9Cgreen%E2%80%9D-wind-turbine-accidents-injuries-and-fatalities-raise-serious-safety-concerns last retrieved on 25/01/2022
[4] https://www.offshore-technology.com/features/feature-the-worlds-deadliest-offshore-oil-rig-disasters-4149812/ last retrieved on 25/01/2022
[5] Broitman E 2016. Tribology Letters **65**(23) 1–18
[6] Bolzon G, Buljak V, Maier G and Miller B 2011 *Inv. Problems Sci Eng*. **19** 815–37
[7] Bolzon G, Molinas B and Talassi M 2012 *Strain* **48** 517–27
[8] EN ISO 6508:2005 Metallic materials – Rockwell hardness test
[9] ASTM E18–20 Standard Test Methods for Rockwell Hardness of Metallic Materials
[10] Ly HV and Tran HT 2001 *Math. Comput. Model* **33** 223–36
[11] Bolzon G, Maier G and Panico M 2004 *Int. J. Solids Struct*. **41** 2957–75